

Search for pair production of scalar bottom quarks in $p\bar{p}$ collisions at $\sqrt{s}=1.96$ TeV

V.M. Abazov,³⁶ B. Abbott,⁷⁶ M. Abolins,⁶⁶ B.S. Acharya,²⁹ M. Adams,⁵² T. Adams,⁵⁰ M. Agelou,¹⁸ S.H. Ahn,³¹ M. Ahsan,⁶⁰ G.D. Alexeev,³⁶ G. Alkhazov,⁴⁰ A. Alton,⁶⁵ G. Alverson,⁶⁴ G.A. Alves,² M. Anastasoae,³⁵ T. Andeen,⁵⁴ S. Anderson,⁴⁶ B. Andrieu,¹⁷ M.S. Anzels,⁵⁴ Y. Arnoud,¹⁴ M. Arov,⁵³ A. Askew,⁵⁰ B. Åsman,⁴¹ A.C.S. Assis Jesus,³ O. Atramentov,⁵⁸ C. Autermann,²¹ C. Avila,⁸ C. Ay,²⁴ F. Badaud,¹³ A. Baden,⁶² L. Bagby,⁵³ B. Baldin,⁵¹ D.V. Bandurin,⁶⁰ P. Banerjee,²⁹ S. Banerjee,²⁹ E. Barberis,⁶⁴ P. Bargassa,⁸¹ P. Baringer,⁵⁹ C. Barnes,⁴⁴ J. Barreto,² J.F. Bartlett,⁵¹ U. Bassler,¹⁷ D. Bauer,⁴⁴ A. Bean,⁵⁹ M. Begalli,³ M. Begel,⁷² C. Belanger-Champagne,⁵ L. Bellantoni,⁵¹ A. Bellavance,⁶⁸ J.A. Benitez,⁶⁶ S.B. Beri,²⁷ G. Bernardi,¹⁷ R. Bernhard,⁴² L. Berntzon,¹⁵ I. Bertram,⁴³ M. Besançon,¹⁸ R. Beuselinck,⁴⁴ V.A. Bezzubov,³⁹ P.C. Bhat,⁵¹ V. Bhatnagar,²⁷ M. Binder,²⁵ C. Biscarat,⁴³ K.M. Black,⁶³ I. Blackler,⁴⁴ G. Blazey,⁵³ F. Blekman,⁴⁴ S. Blessing,⁵⁰ D. Bloch,¹⁹ K. Bloom,⁶⁸ U. Blumenschein,²³ A. Boehnlein,⁵¹ O. Boeriu,⁵⁶ T.A. Bolton,⁶⁰ G. Borissov,⁴³ K. Bos,³⁴ T. Bose,⁷⁸ A. Brandt,⁷⁹ R. Brock,⁶⁶ G. Brooijmans,⁷¹ A. Bross,⁵¹ D. Brown,⁷⁹ N.J. Buchanan,⁵⁰ D. Buchholz,⁵⁴ M. Buehler,⁸² V. Buescher,²³ S. Burdin,⁵¹ S. Burke,⁴⁶ T.H. Burnett,⁸³ E. Busato,¹⁷ C.P. Buszello,⁴⁴ J.M. Butler,⁶³ P. Calfayan,²⁵ S. Calvet,¹⁵ J. Cammin,⁷² S. Caron,³⁴ W. Carvalho,³ B.C.K. Casey,⁷⁸ N.M. Cason,⁵⁶ H. Castilla-Valdez,³³ D. Chakraborty,⁵³ K.M. Chan,⁷² A. Chandra,⁴⁹ F. Charles,¹⁹ E. Cheu,⁴⁶ F. Chevallier,¹⁴ D.K. Cho,⁶³ S. Choi,³² B. Choudhary,²⁸ L. Christofek,⁵⁹ D. Claes,⁶⁸ B. Clément,¹⁹ C. Clément,⁴¹ Y. Coadou,⁵ M. Cooke,⁸¹ W.E. Cooper,⁵¹ D. Coppage,⁵⁹ M. Corcoran,⁸¹ M.-C. Cousinou,¹⁵ B. Cox,⁴⁵ S. Crépe-Renaudin,¹⁴ D. Cutts,⁷⁸ M. Cwiok,³⁰ H. da Motta,² A. Das,⁶³ M. Das,⁶¹ B. Davies,⁴³ G. Davies,⁴⁴ G.A. Davis,⁵⁴ K. De,⁷⁹ P. de Jong,³⁴ S.J. de Jong,³⁵ E. De La Cruz-Burelo,⁶⁵ C. De Oliveira Martins,³ J.D. Degenhardt,⁶⁵ F. Déliot,¹⁸ M. Demarteau,⁵¹ R. Demina,⁷² P. Demine,¹⁸ D. Denisov,⁵¹ S.P. Denisov,³⁹ S. Desai,⁷³ H.T. Diehl,⁵¹ M. Diesburg,⁵¹ M. Doidge,⁴³ A. Dominguez,⁶⁸ H. Dong,⁷³ L.V. Dudko,³⁸ L. Dufflot,¹⁶ S.R. Dugad,²⁹ D. Duggan,⁵⁰ A. Duperrin,¹⁵ J. Dyer,⁶⁶ A. Dyshkant,⁵³ M. Eads,⁶⁸ D. Edmunds,⁶⁶ T. Edwards,⁴⁵ J. Ellison,⁴⁹ J. Elmsheuser,²⁵ V.D. Elvira,⁵¹ S. Eno,⁶² P. Ermolov,³⁸ H. Evans,⁵⁵ A. Evdokimov,³⁷ V.N. Evdokimov,³⁹ S.N. Fatakia,⁶³ L. Feligioni,⁶³ A.V. Ferapontov,⁶⁰ T. Ferbel,⁷² F. Fiedler,²⁵ F. Filthaut,³⁵ W. Fisher,⁵¹ H.E. Fisk,⁵¹ I. Fleck,²³ M. Ford,⁴⁵ M. Fortner,⁵³ H. Fox,²³ S. Fu,⁵¹ S. Fuess,⁵¹ T. Gadfort,⁸³ C.F. Galea,³⁵ E. Gallas,⁵¹ E. Galyaev,⁵⁶ C. Garcia,⁷² A. Garcia-Bellido,⁸³ J. Gardner,⁵⁹ V. Gavrilov,³⁷ A. Gay,¹⁹ P. Gay,¹³ D. Gelé,¹⁹ R. Gelhaus,⁴⁹ C.E. Gerber,⁵² Y. Gershtein,⁵⁰ D. Gillberg,⁵ G. Ginther,⁷² N. Gollub,⁴¹ B. Gómez,⁸ A. Goussiou,⁵⁶ P.D. Grannis,⁷³ H. Greenlee,⁵¹ Z.D. Greenwood,⁶¹ E.M. Gregores,⁴ G. Grenier,²⁰ Ph. Gris,¹³ J.-F. Grivaz,¹⁶ S. Grünendahl,⁵¹ M.W. Grünewald,³⁰ F. Guo,⁷³ J. Guo,⁷³ G. Gutierrez,⁵¹ P. Gutierrez,⁷⁶ A. Haas,⁷¹ N.J. Hadley,⁶² P. Haefner,²⁵ S. Hagopian,⁵⁰ J. Haley,⁶⁹ I. Hall,⁷⁶ R.E. Hall,⁴⁸ L. Han,⁷ K. Hanagaki,⁵¹ K. Harder,⁶⁰ A. Harel,⁷² R. Harrington,⁶⁴ J.M. Hauptman,⁵⁸ R. Hauser,⁶⁶ J. Hays,⁵⁴ T. Hebbeker,²¹ D. Hedin,⁵³ J.G. Hegeman,³⁴ J.M. Heinmiller,⁵² A.P. Heinson,⁴⁹ U. Heintz,⁶³ C. Hensel,⁵⁹ K. Herner,⁷³ G. Hesketh,⁶⁴ M.D. Hildreth,⁵⁶ R. Hirosky,⁸² J.D. Hobbs,⁷³ B. Hoeneisen,¹² H. Hoeth,²⁶ M. Hohlfeld,¹⁶ S.J. Hong,³¹ R. Hooper,⁷⁸ P. Houben,³⁴ Y. Hu,⁷³ Z. Hubacek,¹⁰ V. Hynek,⁹ I. Iashvili,⁷⁰ R. Illingworth,⁵¹ A.S. Ito,⁵¹ S. Jabeen,⁶³ M. Jaffré,¹⁶ S. Jain,⁷⁶ K. Jakobs,²³ C. Jarvis,⁶² A. Jenkins,⁴⁴ R. Jesik,⁴⁴ K. Johns,⁴⁶ C. Johnson,⁷¹ M. Johnson,⁵¹ A. Jonckheere,⁵¹ P. Jonsson,⁴⁴ A. Juste,⁵¹ D. Käfer,²¹ S. Kahn,⁷⁴ E. Kajfasz,¹⁵ A.M. Kalinin,³⁶ J.M. Kalk,⁶¹ J.R. Kalk,⁶⁶ S. Kappler,²¹ D. Karmanov,³⁸ J. Kasper,⁶³ P. Kasper,⁵¹ I. Katsanos,⁷¹ D. Kau,⁵⁰ R. Kaur,²⁷ R. Kehoe,⁸⁰ S. Kermiche,¹⁵ N. Khalatyan,⁶³ A. Khanov,⁷⁷ A. Kharchilava,⁷⁰ Y.M. Khazdzhiev,³⁶ D. Khatidze,⁷¹ H. Kim,⁷⁹ T.J. Kim,³¹ M.H. Kirby,³⁵ B. Klima,⁵¹ J.M. Kohli,²⁷ J.-P. Konrath,²³ M. Kopal,⁷⁶ V.M. Korablev,³⁹ J. Kotcher,⁷⁴ B. Kothari,⁷¹ A. Koubarovsky,³⁸ A.V. Kozelov,³⁹ J. Kozminski,⁶⁶ D. Krop,⁵⁵ A. Kryemadhi,⁸² T. Kuhl,²⁴ A. Kumar,⁷⁰ S. Kunori,⁶² A. Kupco,¹¹ T. Kurča,^{20,*} J. Kvita,⁹ S. Lammers,⁷¹ G. Landsberg,⁷⁸ J. Lazoflores,⁵⁰ A.-C. Le Bihan,¹⁹ P. Lebrun,²⁰ W.M. Lee,⁵³ A. Leflat,³⁸ F. Lehner,⁴² V. Lesne,¹³ J. Leveque,⁴⁶ P. Lewis,⁴⁴ J. Li,⁷⁹ Q.Z. Li,⁵¹ J.G.R. Lima,⁵³ D. Lincoln,⁵¹ J. Linnemann,⁶⁶ V.V. Lipaev,³⁹ R. Lipton,⁵¹ Z. Liu,⁵ L. Lobo,⁴⁴ A. Lobodenko,⁴⁰ M. Lokajicek,¹¹ A. Lounis,¹⁹ P. Love,⁴³ H.J. Lubatti,⁸³ M. Lynker,⁵⁶ A.L. Lyon,⁵¹ A.K.A. Maciel,² R.J. Madaras,⁴⁷ P. Mättig,²⁶ C. Magass,²¹ A. Magerkurth,⁶⁵ A.-M. Magnan,¹⁴ N. Makovec,¹⁶ P.K. Mal,⁵⁶ H.B. Malbouisson,³ S. Malik,⁶⁸ V.L. Malyshev,³⁶ H.S. Mao,⁶ Y. Maravin,⁶⁰ M. Martens,⁵¹ R. McCarthy,⁷³ D. Meder,²⁴ A. Melnitchouk,⁶⁷ A. Mendes,¹⁵ L. Mendoza,⁸ M. Merkin,³⁸ K.W. Merritt,⁵¹ A. Meyer,²¹ J. Meyer,²² M. Michaut,¹⁸ H. Miettinen,⁸¹ T. Millet,²⁰ J. Mitrevski,⁷¹ J. Molina,³ N.K. Mondal,²⁹ J. Monk,⁴⁵ R.W. Moore,⁵ T. Moulik,⁵⁹ G.S. Muanza,¹⁶ M. Mulders,⁵¹ M. Mulhearn,⁷¹ L. Mundim,³ Y.D. Mutaf,⁷³ E. Nagy,¹⁵ M. Naimuddin,²⁸ M. Narain,⁶³ N.A. Naumann,³⁵ H.A. Neal,⁶⁵ J.P. Negret,⁸

P. Neustroev,⁴⁰ C. Noeding,²³ A. Nomerotski,⁵¹ S.F. Novaes,⁴ T. Nunnemann,²⁵ V. O'Dell,⁵¹ D.C. O'Neil,⁵ G. Odrant,⁴⁰ V. Oguri,³ N. Oliveira,³ N. Oshima,⁵¹ R. Otec,¹⁰ G.J. Otero y Garzón,⁵² M. Owen,⁴⁵ P. Padley,⁸¹ N. Parashar,⁵⁷ S.-J. Park,⁷² S.K. Park,³¹ J. Parsons,⁷¹ R. Partridge,⁷⁸ N. Parua,⁷³ A. Patwa,⁷⁴ G. Pawloski,⁸¹ P.M. Perea,⁴⁹ E. Perez,¹⁸ K. Peters,⁴⁵ P. Pétroff,¹⁶ M. Petteni,⁴⁴ R. Piegai,¹ J. Piper,⁶⁶ M.-A. Pleier,²² P.L.M. Podesta-Lerma,³³ V.M. Podstavkov,⁵¹ Y. Pogorelov,⁵⁶ M.-E. Pol,² A. Pomposh,⁷⁶ B.G. Pope,⁶⁶ A.V. Popov,³⁹ C. Potter,⁵ W.L. Prado da Silva,³ H.B. Prosper,⁵⁰ S. Protopopescu,⁷⁴ J. Qian,⁶⁵ A. Quadt,²² B. Quinn,⁶⁷ M.S. Rangel,² K.J. Rani,²⁹ K. Ranjan,²⁸ P.N. Ratoff,⁴³ P. Renkel,⁸⁰ S. Reucroft,⁶⁴ M. Rijssenbeek,⁷³ I. Ripp-Baudot,¹⁹ F. Rizatdinova,⁷⁷ S. Robinson,⁴⁴ R.F. Rodrigues,³ C. Royon,¹⁸ P. Rubinov,⁵¹ R. Ruchti,⁵⁶ V.I. Rud,³⁸ G. Sajot,¹⁴ A. Sánchez-Hernández,³³ M.P. Sanders,⁶² A. Santoro,³ G. Savage,⁵¹ L. Sawyer,⁶¹ T. Scanlon,⁴⁴ D. Schaile,²⁵ R.D. Schamberger,⁷³ Y. Scheglov,⁴⁰ H. Schellman,⁵⁴ P. Schieferdecker,²⁵ C. Schmitt,²⁶ C. Schwanenberger,⁴⁵ A. Schwartzman,⁶⁹ R. Schwienhorst,⁶⁶ J. Sekaric,⁵⁰ S. Sengupta,⁵⁰ H. Severini,⁷⁶ E. Shabalina,⁵² M. Shamim,⁶⁰ V. Shary,¹⁸ A.A. Shchukin,³⁹ W.D. Shephard,⁵⁶ R.K. Shivpuri,²⁸ D. Shpakov,⁵¹ V. Siccaldi,¹⁹ R.A. Sidwell,⁶⁰ V. Simak,¹⁰ V. Sirotenko,⁵¹ P. Skubic,⁷⁶ P. Slattery,⁷² R.P. Smith,⁵¹ G.R. Snow,⁶⁸ J. Snow,⁷⁵ S. Snyder,⁷⁴ S. Söldner-Rembold,⁴⁵ X. Song,⁵³ L. Sonnenschein,¹⁷ A. Sopczak,⁴³ M. Sosebee,⁷⁹ K. Soustruznik,⁹ M. Souza,² B. Spurlock,⁷⁹ J. Stark,¹⁴ J. Steele,⁶¹ V. Stolin,³⁷ A. Stone,⁵² D.A. Stoyanova,³⁹ J. Strandberg,⁴¹ S. Strandberg,⁴¹ M.A. Strang,⁷⁰ M. Strauss,⁷⁶ R. Ströhmer,²⁵ D. Strom,⁵⁴ M. Strovink,⁴⁷ L. Stutte,⁵¹ S. Sumowidagdo,⁵⁰ A. Sznajder,³ M. Talby,¹⁵ P. Tamburello,⁴⁶ W. Taylor,⁵ P. Telford,⁴⁵ J. Temple,⁴⁶ B. Tiller,²⁵ M. Titov,²³ V.V. Tokmenin,³⁶ M. Tomoto,⁵¹ T. Toole,⁶² I. Torchiani,²³ S. Towers,⁴³ T. Trefzger,²⁴ S. Trincaz-Duvold,¹⁷ D. Tsybychev,⁷³ B. Tuchming,¹⁸ C. Tully,⁶⁹ A.S. Turcot,⁴⁵ P.M. Tuts,⁷¹ R. Unalan,⁶⁶ L. Uvarov,⁴⁰ S. Uvarov,⁴⁰ S. Uzunyan,⁵³ B. Vachon,⁵ P.J. van den Berg,³⁴ R. Van Kooten,⁵⁵ W.M. van Leeuwen,³⁴ N. Varelas,⁵² E.W. Varnes,⁴⁶ A. Vartapetian,⁷⁹ I.A. Vasilyev,³⁹ M. Vaupel,²⁶ P. Verdier,²⁰ L.S. Vertogradov,³⁶ M. Verzocchi,⁵¹ F. Villeneuve-Seguié,⁴⁴ P. Vint,⁴⁴ J.-R. Vlimant,¹⁷ E. Von Toerne,⁶⁰ M. Voutilainen,^{68,†} M. Vreeswijk,³⁴ H.D. Wahl,⁵⁰ L. Wang,⁶² M.H.L.S Wang,⁵¹ J. Warchol,⁵⁶ G. Watts,⁸³ M. Wayne,⁵⁶ M. Weber,⁵¹ H. Weerts,⁶⁶ N. Wermes,²² M. Wetstein,⁶² A. White,⁷⁹ D. Wicke,²⁶ G.W. Wilson,⁵⁹ S.J. Wimpenny,⁴⁹ M. Wobisch,⁵¹ J. Womersley,⁵¹ D.R. Wood,⁶⁴ T.R. Wyatt,⁴⁵ Y. Xie,⁷⁸ N. Xuan,⁵⁶ S. Yacoob,⁵⁴ R. Yamada,⁵¹ M. Yan,⁶² T. Yasuda,⁵¹ Y.A. Yatsunenko,³⁶ K. Yip,⁷⁴ H.D. Yoo,⁷⁸ S.W. Youn,⁵⁴ C. Yu,¹⁴ J. Yu,⁷⁹ A. Yurkewicz,⁷³ A. Zatserklyaniy,⁵³ C. Zeitnitz,²⁶ D. Zhang,⁵¹ T. Zhao,⁸³ B. Zhou,⁶⁵ J. Zhu,⁷³ M. Zielinski,⁷² D. Zieminska,⁵⁵ A. Zieminski,⁵⁵ V. Zutshi,⁵³ and E.G. Zverev³⁸

(DØ Collaboration)

¹Universidad de Buenos Aires, Buenos Aires, Argentina

²LAFEX, Centro Brasileiro de Pesquisas Físicas, Rio de Janeiro, Brazil

³Universidade do Estado do Rio de Janeiro, Rio de Janeiro, Brazil

⁴Instituto de Física Teórica, Universidade Estadual Paulista, São Paulo, Brazil

⁵University of Alberta, Edmonton, Alberta, Canada, Simon Fraser University, Burnaby, British Columbia, Canada, York University, Toronto, Ontario, Canada, and McGill University, Montreal, Quebec, Canada

⁶Institute of High Energy Physics, Beijing, People's Republic of China

⁷University of Science and Technology of China, Hefei, People's Republic of China

⁸Universidad de los Andes, Bogotá, Colombia

⁹Center for Particle Physics, Charles University, Prague, Czech Republic

¹⁰Czech Technical University, Prague, Czech Republic

¹¹Center for Particle Physics, Institute of Physics, Academy of Sciences of the Czech Republic, Prague, Czech Republic

¹²Universidad San Francisco de Quito, Quito, Ecuador

¹³Laboratoire de Physique Corpusculaire, IN2P3-CNRS, Université Blaise Pascal, Clermont-Ferrand, France

¹⁴Laboratoire de Physique Subatomique et de Cosmologie, IN2P3-CNRS, Université de Grenoble 1, Grenoble, France

¹⁵CPPM, IN2P3-CNRS, Université de la Méditerranée, Marseille, France

¹⁶IN2P3-CNRS, Laboratoire de l'Accélérateur Linéaire, Orsay, France

¹⁷LPNHE, IN2P3-CNRS, Universités Paris VI and VII, Paris, France

¹⁸DAPNIA/Service de Physique des Particules, CEA, Saclay, France

¹⁹IPHC, IN2P3-CNRS, Université Louis Pasteur, Strasbourg, France, and Université de Haute Alsace, Mulhouse, France

²⁰Institut de Physique Nucléaire de Lyon, IN2P3-CNRS, Université Claude Bernard, Villeurbanne, France

²¹III. Physikalisches Institut A, RWTH Aachen, Aachen, Germany

²²Physikalisches Institut, Universität Bonn, Bonn, Germany

²³Physikalisches Institut, Universität Freiburg, Freiburg, Germany

²⁴Institut für Physik, Universität Mainz, Mainz, Germany

²⁵Ludwig-Maximilians-Universität München, München, Germany

²⁶Fachbereich Physik, University of Wuppertal, Wuppertal, Germany

²⁷Panjab University, Chandigarh, India

- ²⁸ Delhi University, Delhi, India
- ²⁹ Tata Institute of Fundamental Research, Mumbai, India
- ³⁰ University College Dublin, Dublin, Ireland
- ³¹ Korea Detector Laboratory, Korea University, Seoul, Korea
- ³² SungKyunKwan University, Suwon, Korea
- ³³ CINVESTAV, Mexico City, Mexico
- ³⁴ FOM-Institute NIKHEF and University of Amsterdam/NIKHEF, Amsterdam, The Netherlands
- ³⁵ Radboud University Nijmegen/NIKHEF, Nijmegen, The Netherlands
- ³⁶ Joint Institute for Nuclear Research, Dubna, Russia
- ³⁷ Institute for Theoretical and Experimental Physics, Moscow, Russia
- ³⁸ Moscow State University, Moscow, Russia
- ³⁹ Institute for High Energy Physics, Protvino, Russia
- ⁴⁰ Petersburg Nuclear Physics Institute, St. Petersburg, Russia
- ⁴¹ Lund University, Lund, Sweden, Royal Institute of Technology and Stockholm University, Stockholm, Sweden, and Uppsala University, Uppsala, Sweden
- ⁴² Physik Institut der Universität Zürich, Zürich, Switzerland
- ⁴³ Lancaster University, Lancaster, United Kingdom
- ⁴⁴ Imperial College, London, United Kingdom
- ⁴⁵ University of Manchester, Manchester, United Kingdom
- ⁴⁶ University of Arizona, Tucson, Arizona 85721, USA
- ⁴⁷ Lawrence Berkeley National Laboratory and University of California, Berkeley, California 94720, USA
- ⁴⁸ California State University, Fresno, California 93740, USA
- ⁴⁹ University of California, Riverside, California 92521, USA
- ⁵⁰ Florida State University, Tallahassee, Florida 32306, USA
- ⁵¹ Fermi National Accelerator Laboratory, Batavia, Illinois 60510, USA
- ⁵² University of Illinois at Chicago, Chicago, Illinois 60607, USA
- ⁵³ Northern Illinois University, DeKalb, Illinois 60115, USA
- ⁵⁴ Northwestern University, Evanston, Illinois 60208, USA
- ⁵⁵ Indiana University, Bloomington, Indiana 47405, USA
- ⁵⁶ University of Notre Dame, Notre Dame, Indiana 46556, USA
- ⁵⁷ Purdue University Calumet, Hammond, Indiana 46323, USA
- ⁵⁸ Iowa State University, Ames, Iowa 50011, USA
- ⁵⁹ University of Kansas, Lawrence, Kansas 66045, USA
- ⁶⁰ Kansas State University, Manhattan, Kansas 66506, USA
- ⁶¹ Louisiana Tech University, Ruston, Louisiana 71272, USA
- ⁶² University of Maryland, College Park, Maryland 20742, USA
- ⁶³ Boston University, Boston, Massachusetts 02215, USA
- ⁶⁴ Northeastern University, Boston, Massachusetts 02115, USA
- ⁶⁵ University of Michigan, Ann Arbor, Michigan 48109, USA
- ⁶⁶ Michigan State University, East Lansing, Michigan 48824, USA
- ⁶⁷ University of Mississippi, University, Mississippi 38677, USA
- ⁶⁸ University of Nebraska, Lincoln, Nebraska 68588, USA
- ⁶⁹ Princeton University, Princeton, New Jersey 08544, USA
- ⁷⁰ State University of New York, Buffalo, New York 14260, USA
- ⁷¹ Columbia University, New York, New York 10027, USA
- ⁷² University of Rochester, Rochester, New York 14627, USA
- ⁷³ State University of New York, Stony Brook, New York 11794, USA
- ⁷⁴ Brookhaven National Laboratory, Upton, New York 11973, USA
- ⁷⁵ Langston University, Langston, Oklahoma 73050, USA
- ⁷⁶ University of Oklahoma, Norman, Oklahoma 73019, USA
- ⁷⁷ Oklahoma State University, Stillwater, Oklahoma 74078, USA
- ⁷⁸ Brown University, Providence, Rhode Island 02912, USA
- ⁷⁹ University of Texas, Arlington, Texas 76019, USA
- ⁸⁰ Southern Methodist University, Dallas, Texas 75275, USA
- ⁸¹ Rice University, Houston, Texas 77005, USA
- ⁸² University of Virginia, Charlottesville, Virginia 22901, USA
- ⁸³ University of Washington, Seattle, Washington 98195, USA

(Dated: August 7, 2006)

A search for direct production of scalar bottom quarks (\bar{b}) is performed with 310 pb^{-1} of data collected by the DØ experiment in $p\bar{p}$ collisions at $\sqrt{s} = 1.96 \text{ TeV}$ at the Fermilab Tevatron Collider. The topology analyzed consists of two b jets and an imbalance in transverse momentum due to undetected neutralinos ($\tilde{\chi}_1^0$), with $\tilde{\chi}_1^0$ assumed to be the lightest supersymmetric particle. We find

the data consistent with standard model expectations, and set a 95% C.L. exclusion domain in the $(m_{\tilde{b}}, m_{\tilde{\chi}_1^0})$ mass plane, improving significantly upon the results from Run I of the Tevatron.

PACS numbers: 14.80.Ly, 12.60.Jv, 13.85.Rm

Supersymmetric (SUSY) models [1] provide an extension of the standard model (SM) with mechanisms viable for the unification of interactions and a solution to the hierarchy problem. Particularly attractive are models that conserve R -parity, in which SUSY particles are produced in pairs and the lightest supersymmetric particle (LSP) is stable. In SUSY, a scalar field is associated to each of the left and right handed chirality states of a given SM quark or lepton. Two mass eigenstates result from the mixing of these scalar fields. The spin-1/2 partners of the neutral gauge and Higgs bosons are called neutralinos.

In supergravity inspired models [2], the lightest neutralino $\tilde{\chi}_1^0$ arises as the natural LSP, and, being neutral and weakly interacting, could be responsible for the dark matter in the universe. For large values of $\tan\beta$ (the ratio of the vacuum expectation values of the two Higgs fields) the mixing term among the scalar fields associated with the bottom quark is large. Therefore, a large splitting is expected among the mass eigenstates, that could result in a low mass value for one of them, hereafter called scalar bottom quark or sbottom (\tilde{b}). The SUSY particle mass hierarchy can even be such that the decay $\tilde{b} \rightarrow b\tilde{\chi}_1^0$ is the only one kinematically allowed [3], an assumption that is made in the following.

In this Letter, a search is reported for \tilde{b} pair production with 310 pb^{-1} of data collected during Run II of the Fermilab Tevatron. At leading order, the \tilde{b} pair production cross section in $p\bar{p}$ collisions depends only on the sbottom mass. For a center-of-mass energy $\sqrt{s} = 1.96 \text{ TeV}$, the next-to-leading order (NLO) cross section, calculated with PROSPINO-2 [4] ranges from 15 to 0.084 pb for sbottom masses between 100 and 230 GeV, with very little dependence on the masses of the other SUSY particles. The final state of this process corresponds to two b jets and missing transverse energy (\cancel{E}_T) due to the undetected neutralinos. The maximum sbottom mass ($m_{\tilde{b}}$) excluded by previous results is 148 GeV [5].

A full description of the DØ detector is available in Ref. [6]. The central tracking system consists of a silicon microstrip tracker and a central fiber tracker, both located within a 1.9 T superconducting solenoid. A liquid-argon and uranium calorimeter covers pseudorapidities up to $|\eta| \approx 4.2$, where $\eta = -\ln[\tan(\theta/2)]$ and θ is the polar angle relative to the proton beam. The calorimeter has three sections, housed in separate cryostats: the central one covers $|\eta| \lesssim 1.1$, and the two end sections extend the coverage to larger $|\eta|$. The calorimeter is segmented in depth, with four electromagnetic layers followed by up to five hadronic layers. It is also segmented into projective towers of 0.1×0.1 size in $\eta - \phi$ space, where ϕ

is the azimuth in radians. An outer muon system, covering $|\eta| < 2$, consists of a layer of tracking detectors and scintillation trigger counters positioned in front of 1.8 T toroids, followed by two similar layers after the toroids. Jet reconstruction is based on the Run II cone algorithm [7] with a cone size of 0.5, that uses energies deposited in calorimeter towers. Jet energies are calibrated using transverse momentum balance in photon+jet events. The missing transverse energy in an event is based on all calorimeter cells, and is corrected for the jet energy calibration and for reconstructed muons.

The DØ trigger has three levels: L1, L2, and L3. The data were collected with triggers specifically designed for \cancel{E}_T +jets topologies. We define $\cancel{E}_T = |\sum_{\text{jets}} \vec{p}_T^j|$ the vector sum of the jet transverse momenta. The trigger conditions at L1 require at least three calorimeter towers with $E_T > 5 \text{ GeV}$, where a trigger tower spans $\Delta\phi \times \Delta\eta = 0.2 \times 0.2$. We then require $\cancel{E}_T > 20$ (30) GeV at L2 (L3). Approximately 14 million events were collected with the \cancel{E}_T +jets triggers.

The signal is simulated in the framework of a generic minimal supersymmetric standard model, in which we vary the masses of the \tilde{b} and $\tilde{\chi}_1^0$, all other parameters being fixed. The masses of the other SUSY particles are set such that the only sbottom decay mode is into $b\tilde{\chi}_1^0$. The SUSY and SM processes are processed using Monte Carlo (MC) generators PYTHIA 6.202 [8] for the signal, ALPGEN 1.3.3 [9] interfaced with PYTHIA for the SM. All the events are passed through a full GEANT-3 [10] simulation of the geometry and response of the DØ detector with an average of 0.8 minimum-bias events overlaid on each generated event. The CTEQ5L parton density functions (PDF) [11] are used in the simulation.

Instrumental background from mismeasurement of jet energies in multijet events is estimated from data, and is referred to as “QCD” background in the following. The main SM backgrounds relevant to our analysis are from vector boson production in association with jets, and top quark production. To estimate the backgrounds from W/Z +jets processes, we use the NLO cross sections computed with MCFM [12]. The theoretical NNLO $t\bar{t}$ production cross section is taken from Ref. [13].

The events are examined to ensure that the reconstructed vertex corresponds to the actual position of the primary vertex (PV). We select events that are well contained in the detector by restricting the PV within 60 cm along the beam direction with respect to the detector center. We define a charged-particle fraction (CPF) as the ratio of the charged-particle transverse energy, computed from the sum of scalar p_T values of charged parti-

cles (reconstructed in the tracking system) that emanate from the PV and are associated with a jet, divided by the jet transverse energy measured in the calorimeter. The two leading jets, i.e those with the largest transverse energies, are required to have $\text{CPF} > 0.05$. This criterion rejects events with fake jets or where a wrong PV is selected. The overall inefficiency associated with this procedure is measured using events collected at random beam crossings, and events with two jets emitted back-to-back in azimuth. The jets must also have energy fraction in the electromagnetic layers of the calorimeter < 0.95 and $p_T > 30, 15$ GeV for the first and second leading jets. This set of initial cuts requires in addition $\Delta\phi < 165^\circ$, where $\Delta\phi$ is defined as the difference in azimuth between the two leading jets.

Table I defines our selection criteria, and shows the effect of applying them sequentially in the analysis of data, and their impact on signal efficiency, for the choice of $(m_{\tilde{b}}, m_{\tilde{\chi}_1^0}) = (140, 80)$ GeV. Criteria **C1-C4** are effective against QCD, **C2** and **C4-C8** against vector-bosons+jets, and **C9** suppresses $t\bar{t}$ background. For \tilde{b} masses of ~ 100 GeV, the mean \cancel{E}_T and jet p_T are close to what is expected from SM backgrounds, but are substantially larger for higher \tilde{b} masses. The selections are tuned on MC so as to maintain good sensitivity to signal for small \tilde{b} masses, using minimal values for threshold requirements, for instance $\cancel{E}_T > 60$ GeV (**C1**) and $p_T > 40, 20$ GeV (**C2**) for the first and second leading jets. Later we show that, depending on the masses $(m_{\tilde{b}}, m_{\tilde{\chi}_1^0})$, higher thresholds on \cancel{E}_T and jet p_T can be applied to increase the sensitivity to signal.

The first and second leading jets are required to be in the central region of the calorimeter, $|\eta^{\text{det}}| < 1.1$ and 2.0 respectively (**C3**), where η^{det} is the jet pseudorapidity calculated with a jet origin at the detector center. Because of the central production of \tilde{b} events, these selections do not affect signal efficiency, but reduce background. We also define $\Delta\phi_{\min}(\cancel{E}_T, \text{jets})$ and $\Delta\phi_{\max}(\cancel{E}_T, \text{jets})$, the minimum and maximum of the differences in azimuth between the direction of \cancel{E}_T and the direction of any jet. Requiring $\Delta\phi_{\min} > 35^\circ$ rejects QCD events (**C4**), and $\Delta\phi_{\min} < 120^\circ$ and $\Delta\phi_{\max} < 175^\circ$ suppress SM background (**C4, C5**).

Since we do not expect isolated electrons, muons or tau leptons in signal events, vetoes are imposed on events with an isolated electron (**C6**), muon (**C7**), or a charged track (**C8**) with $p_T > 5$ GeV. Electrons and muons are defined isolated based on a criterion for energy deposition in a cone around the lepton direction in the calorimeter. A charged track is considered isolated if no other charged track with $p_T > 1.5$ GeV is found in a hollow cone with inner and outer radii 0.05 and 0.2, formed around the direction of the track. The last requirement (**C9**) stipulates that either two or three jets are allowed.

Table II gives the numbers of events expected for SM backgrounds and signal, and the number of events ob-

TABLE I: Sequence of criteria applied for the selection of events with their corresponding impact on data and on signal efficiency (Eff.) for $(m_{\tilde{b}}, m_{\tilde{\chi}_1^0}) = (140, 80)$.

Selection criterion applied	Events left	Eff. (%)
C1 : $\cancel{E}_T > 60$ GeV	16,279	18
C2 : $p_{T1} > 40$ GeV, $p_{T2} > 20$ GeV	14,095	16
C3 : $ \eta_{\text{jet}1}^{\text{det}} < 1.1, \eta_{\text{jet}2}^{\text{det}} < 2.0$	9,653	14
C4 : $35^\circ < \Delta\phi_{\min}(\cancel{E}_T, \text{jets}) < 120^\circ$	3,149	10
C5 : $\Delta\phi_{\max}(\cancel{E}_T, \text{jets}) < 175^\circ$	2,783	9
C6 : isolated electron veto	2,059	9
C7 : isolated muon veto	1,809	9
C8 : isolated track veto	756	7
C9 : 2 or 3 jets	671	6

served in data after the above selections. Since an important fraction of the background corresponds to processes with light-flavor jets in the final state, we take advantage of the presence of b jets in the signal to significantly increase the sensitivity of the search by using a lifetime-based heavy-flavor tagging algorithm (b -tagging). Based on the impact parameters of the tracks in the jet, the algorithm [14] computes a probability for a jet to be light-flavored.

We select the b -tagging probability such that 0.1% of the light-flavored jets are tagged for jets having p_T of 50 GeV as yielding the best expected signal sensitivity. The corresponding typical tagging efficiencies for c - and b -quark jets are 5% and 30%, respectively. Because the current detector simulation does not reproduce the tracking precisely enough, the b -tagging algorithm is not applied to simulated jets directly. Instead, jets are weighted by their probability to be b -tagged, according to their flavor, using parameterizations derived from data. In what follows, we require at least one b -tagged jet in the event. Requiring more than one b -tagged jet would lower slightly the sensitivity of the analysis.

In order to estimate the background from QCD, we compare our selected data sample, without imposing the criterion on \cancel{E}_T (**C1**), to the simulation of background from SM. Figure 1 shows that data are well reproduced by the SM background at high \cancel{E}_T . We therefore attribute the exponential rise at low \cancel{E}_T to QCD multijet instrumental background. A fit by an exponential to the data for $\cancel{E}_T < 60$ GeV, after subtraction of the contributions from the SM, is shown in the insert in Fig. 1. When the fit is extrapolated to $\cancel{E}_T > 60$ GeV, it provides an estimate of 109 ± 9 QCD events. After b -tagging, this procedure estimates the presence of only 4 ± 2 events. Given the larger \cancel{E}_T threshold we use for higher sbottom masses, we expect that, after the b -tagging, less than two QCD events will survive the final event selection. The QCD contribution is therefore neglected in the rest of this analysis. Table II shows the results after all selections, including b -tagging, for SM backgrounds, data and signal.

As already mentioned, the mean \cancel{E}_T and jet p_T become

TABLE II: Numbers of events expected from SM and QCD backgrounds, of data events observed, and of signal events expected, after all selection criteria, both before (N_{exp}) and after b -tagging. All uncertainties are statistical only. Backgrounds from b , c , and light jets (j) are shown separately.

SM process	N_{exp}	with b -tagging
$W(e\nu + \mu\nu) + jj$	155 ± 13	1.9 ± 0.2
$W(e\nu + \mu\nu) + cj$	2.2 ± 0.6	0.2 ± 0.1
$W(e\nu + \mu\nu) + b\bar{b}$	1.1 ± 0.1	0.6 ± 0.1
$W(\tau\nu) + \geq 1$ jet	101 ± 14	4.1 ± 0.6
$W(\tau\nu) + b\bar{b}$	2.2 ± 0.3	1.0 ± 0.1
$Z(\nu\bar{\nu}) + jj$	257 ± 12	3.9 ± 0.2
$Z(\nu\bar{\nu}) + c\bar{c}$	8.0 ± 0.7	0.9 ± 0.1
$Z(\nu\bar{\nu}) + b\bar{b}$	7.8 ± 0.3	4.0 ± 0.2
WW, WZ, ZZ	14.2 ± 0.7	0.9 ± 0.2
top production	7.9 ± 0.2	3.8 ± 0.2
Total SM	556 ± 23	21.5 ± 0.8
QCD background	109 ± 9	4 ± 2
Data	671	22
$(m_{\tilde{b}}, m_{\tilde{\chi}_1^0}) = (140, 80)$ GeV	43 ± 2	23.1 ± 0.9

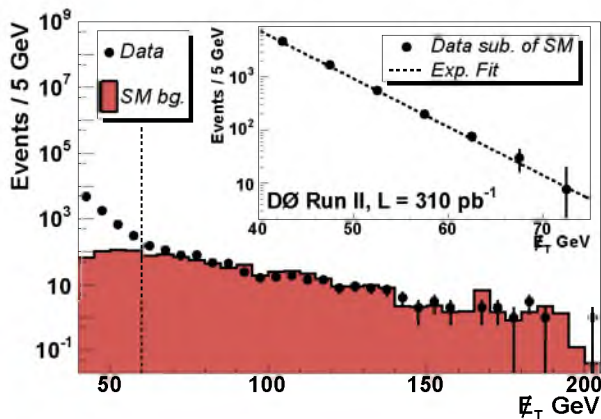


FIG. 1: Distribution in E_T after applying all criteria, except $E_T > 60$ GeV (C1). The dark shaded area corresponds to the SM simulation. A fit by an exponential to $E_T < 60$ GeV, after subtraction of the contributions from the SM, shown in the figure insert, is used to estimate the instrumental background.

substantially larger for higher sbottom masses than the values expected from SM backgrounds. This provides a handle for improving the sensitivity to the signal for large $m_{\tilde{b}}$. Table III shows results for two higher sbottom-mass points, the chosen E_T and p_T thresholds, together with the resulting number of events found after all selections, including b -tagging, for data, SM background and signal. For the highest sbottom masses probed, we note a deficit in the number of events observed compared to the SM background expectation. The probability of such a deficit is 4%.

The following systematic uncertainties are taken into account in deriving the final results. The integrated lu-

TABLE III: Optimized values for the criteria C1 and C2, numbers of data events observed, numbers of events expected from SM and signal for two $(m_{\tilde{b}}, m_{\tilde{\chi}_1^0})$ masses after b -tagging (statistical uncertainties only).

$(m_{\tilde{b}}, m_{\tilde{\chi}_1^0})$ in GeV	(180,90)	(215,0)
C1: E_T [GeV]	60	80
C2: jet 1 p_T [GeV]	70	100
C2: jet 2 p_T [GeV]	40	50
data	7	0
SM	8.9 ± 0.3	3.2 ± 0.2
signal	9.4 ± 0.3	4.6 ± 0.1

minosity contributes an uncertainty of 6.5%. The uncertainty from jet energy calibration is typically of the order of 7%. The total uncertainty from jet energy resolution, jet track confirmation, misvertexing and jet reconstruction is 5%. The systematic uncertainties from NLO cross sections in the SM backgrounds are estimated to be 15%. The effect of the choice of PDF on signal efficiencies is evaluated using the CTEQ6.1M PDF error set [15] resulting in a 8% uncertainty. The uncertainty from MC statistics can reach 10% for the SM and 5% for signal. The total uncertainty from isolated electron, muon, and track vetoes is 9%. The uncertainty from heavy-flavor tagging is 12% for SM and 8% for signal. Finally, the uncertainty from the trigger efficiency is 5%.

Since we do not observe any excess in the data relative to the expectations from SM backgrounds, we set limits on the production of sbottom quarks. Observed and expected 95% confidence level (C.L.) cross section upper limits are obtained using the modified frequentist approach [16], with correlations included between systematic uncertainties. The NLO $\tilde{b}\bar{b}$ pair production cross section is subject to theoretical uncertainties arising from the PDF and from the renormalization and factorization scale choices. For a \tilde{b} mass of 200 GeV, a 16% PDF uncertainty is evaluated using the CTEQ6.1M PDF error set, and a 12% uncertainty is found by varying the scale by a factor of two up or down. For a given neutralino mass, a sbottom mass limit is obtained where the cross section upper limit intersects the production cross section reduced by these uncertainties combined in quadrature. The results are summarized in the 95% C.L. exclusion contours displayed in Fig. 2. At higher sbottom masses, no events are observed where about three are expected, leading to an observed limit more constraining than expected.

In summary, this analysis represents the first Tevatron Run II search for pair production of scalar bottom quarks. The exclusion contour we obtain is substantially more restrictive than the ones published with Run I Tevatron data. With the current analysis using 310 pb^{-1} , the maximum $m_{\tilde{b}}$ excluded is 222 GeV, an improvement of more than 70 GeV with respect to

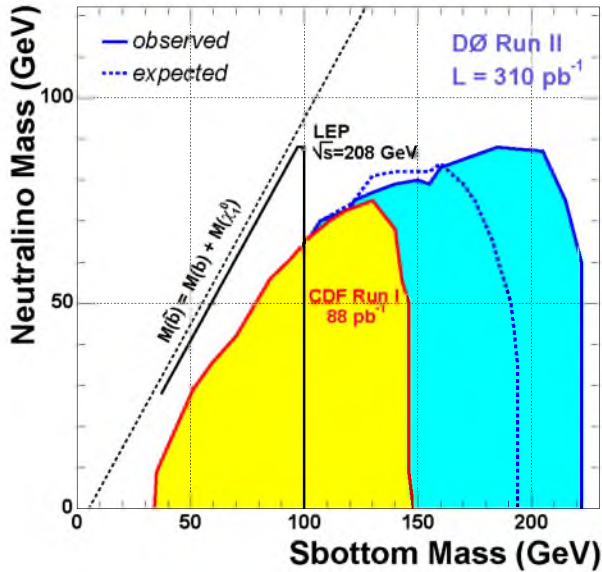


FIG. 2: Excluded regions at the 95% C.L. in the sbottom and neutralino mass plane. The new region excluded by this analysis is shown in dark shading. The dashed line corresponds to the expected limit. Regions excluded by previous experiments are also displayed in the figure [5].

previous results, and the most restrictive limit on the sbottom mass to date.

We thank the staffs at Fermilab and collaborating institutions, and acknowledge support from the DOE and NSF (USA); CEA and CNRS/IN2P3 (France); FASI, Rosatom and RFBR (Russia); CAPES, CNPq, FAPERJ, FAPESP and FUNDUNESP (Brazil); DAE and DST (India); Colciencias (Colombia); CONACyT (Mexico); KRF and KOSEF (Korea); CONICET and UBACyT (Argentina); FOM (The Netherlands); PPARC (United Kingdom); MSMT (Czech Republic); CRC Program, CFI, NSERC and WestGrid Project (Canada); BMBF and DFG (Germany); SFI (Ireland); The Swedish Research Council (Sweden); Research Corporation; Alexan-

der von Humboldt Foundation; and the Marie Curie Program.

-
- [*] On leave from IEP SAS Kosice, Slovakia.
[†] Visitor from Helsinki Institute of Physics, Helsinki, Finland.
- [1] H.E. Haber and G.L. Kane, *Phys. Rep.* **117**, 75 (1985).
[2] H.P. Nilles, *Phys. Rep.* **110**, 1 (1984).
[3] A. Bartl, W. Majerotto and W. Porod, *Z. Phys. C* **64**, 499 (1994), and Erratum *ibid.* **C68**, 518 (1995).
[4] W. Beenakker *et al.*, *Nucl. Phys.* **B515**, 3 (1998).
[5] DØ Collaboration, V. Abazov *et al.*, *Phys. Rev. D Rapid Comm.* **60**, 031101 (1999).
CDF Collaboration, T. Affolder *et al.*, *Phys. Rev. Lett.* **84**, 5704 (2000).
LEPSUSYWG, ALEPH, DELPHI, L3 and OPAL Collaborations, note LEPSUSYWG/04-02.1
<http://lepsusy.web.cern.ch/lepsusy>
[6] DØ Collaboration, V. Abazov *et al.*, *Nucl. Instrum. and Methods A* **565**, 463 (2006).
[7] G.C. Blazey *et al.*, in *Proceedings of the Workshop: "QCD and Weak Boson Physics in Run II,"* edited by U. Baur, R.K. Ellis, and D.Zeppenfeld (Fermilab, Batavia, IL, 2000), p. 47; see Sec. 3.5 for details.
[8] T. Sjöstrand *et al.*, *Comput. Phys. Commun.* **135**, 238 (2001).
[9] M.L. Mangano *et al.*, *J. High Energy Phys.* **0307**, 001 (2003).
[10] R. Brun and F. Carminati, CERN Program Library Long Writeup W5013, 1993 (unpublished).
[11] H.L. Lai *et al.*, *Eur. Phys. J. C* **12**, 375 (2000).
[12] J. Campbell and R. K. Ellis, *Phys. Rev. D* **60**, 113006 (1999).
[13] N. Kidonakis and R. Vogt, *Eur. Phys. J. C* **33**, S466-S468 (2004).
[14] B. Clément, Ph.D. thesis, Université Louis Pasteur, Strasbourg, N° d'ordre IPHC 06-004, N° d'ordre ULP 5086, FERMILAB-THESIS-2006-06 (2006).
[15] J. Pumplin *et al.*, *JHEP* **0207**, 012 (2002); D. Stump *et al.*, *ibid.* **0310**, 046 (2003).
[16] T. Junk, *Nucl. Instrum. Methods A* **434**, 435 (1999); A. Read, in *"First Workshop on Confidence Limits"*, CERN Report No. CERN-2000-005, 2000.